THIEME OPEN ACCESS

Aromatic Residue Positioning Influences Helical Peptoid Structure in Aqueous Solution

Jwwad M. Javed◊
Katherine Scukas◊
Michelle T. Nguyen
Amelia A. Fuller

Department of Chemistry and Biochemistry, Santa Clara University,
500 El Camino Real, Santa Clara, CA 95053, USA
aafuller@scu.edu

◊ These authors contributed equally

Published as part of the Cluster
Chemical Tools for Peptide Modifications

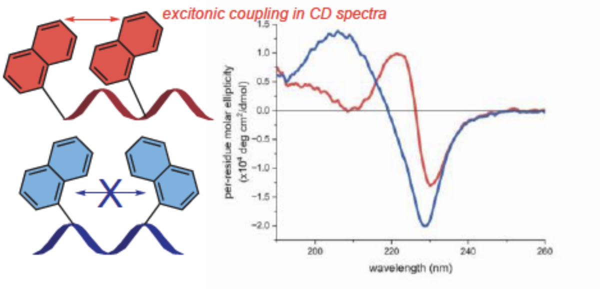

Received: 06.10.2023
Accepted after revision: 29.12.2023
Published online: 04.01.2024 (Accepted Manuscript), 30.01.2024 (Version of Record)
DOI: 10.1055/a-2238-5394; Art ID: ST-2023-10-0451-L

License terms:

© 2024. The Author(s). This is an open access article published by Thieme under the terms of the Creative Commons Attribution License, permitting unrestricted use, distribution and reproduction, so long as the original work is properly cited. (https://creativecommons.org/licenses/by/4.0/)

Abstract Water-soluble peptidomimetics, including peptoids, are promising functional surrogates for biologically relevant, amphiphilic, helical peptides. Twenty amphiphilic peptoid hexamers with predicted helical structures were designed, prepared, and studied using circular dichroism (CD) spectroscopy. The site-specific contributions of aromatic and charged residues to the helical structure of peptoid hexamers in aqueous solution was evaluated, revealing that aromatic residue positioning most significantly impacts structure.

Key words peptoid, peptidomimetic, helical structures, circular dichroism spectroscopy, solid-phase synthesis

Peptoids (*N*-substituted glycine oligomers) have many advantages that enable their widespread study and application as biomimetic scaffolds. The sequence-specific synthesis of monodisperse peptoid analogues bearing peptide-like functional groups is inexpensive and efficient.[1,2] Moreover, peptoids can overcome peptides' pharmacokinetic liabilities: peptoids exhibit proteolytic stability,[3] are not immunogenic,[4] and have useful cell permeability properties.[5] Importantly, peptoids that emulate conformational features of peptides, including helices,[6–12] sheets,[13] and turns,[14] have been described as well as peptoids that adopt abiological folds.[15–17] Of these, a peptoid helix that resembles the polyproline type I (PPI) helix[6] is among the most well-studied structures. Water-soluble PPI helical peptoids have found application as antimicrobials,[18–20] for example, and modulating the secondary structure has been shown to impact the selectivity for bacterial cells over eukaryotic cells.[19] An understanding of how to design and tune peptoid conformations in water is essential to expand peptoids' functional biomimicry.

Inducing peptoid three-dimensional structure, including PPI helical structure, originates from controlling backbone dihedral angles.[21,22] Choice of *N*-substituent (side chain) influences the peptoid backbone amide bond (☐) conformation (Figure 1), and ☐ in turn can promote structure, including the all-*cis*-amide PPI helix. Model peptoid monomers bearing the chiral 1-naphthylethyl side chain favor the *cis* conformation ($K_{cis/trans}$ of 6.27 in CD_3CN) to minimize steric repulsion between the bulky *N*-substituent and the adjacent (*i* – 1) backbone methylene.[21] Tertiary ammonium (*N*,*N*-disubstituted)-2-aminoethyl side chains also favor the *cis*-amide ($K_{cis/trans}$ as high as 8.1 in D_2O).[23] For these residues, the *cis*-amide conformation minimizes unfavorable steric interactions and allows intramolecular H-bonds between the side chain and both the *i* and *i* – 1 carbonyl oxygens.[23] Inclusion of strong *cis*-amide-promoting residues is an effective design strategy for generating PPI helical peptoids.[11]

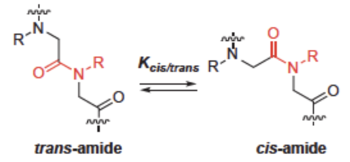

Figure 1 Peptoid structure relies on controlling amide bond (·) conformation by varying the *N*-substituent. PPI helical peptoids comprise *cis*-amide bonds.

In this work, we sought to clarify the position-specific contributions of peptoid residues to amphiphilic PPI helix structure in aqueous solution. High-resolution structural studies of linear peptoids are few;[6,7,11] peptoid secondary structure in solution is commonly inferred from comparative studies of peptoids' circular dichroism (CD) spectra. In organic solution, the site-specific effects of helix-promoting aliphatic and aromatic residues on the solution structures of peptoid PPI helical hexamers[24] and heptamers,[25] respectively, have been explored. In both of these studies, the *C*-terminal residue strongly influenced the peptoid PPI helix structure. However, analogous studies to understand position-specific sequence–structure relationships in water-soluble peptoids are underdeveloped – the helical modulation of 12-residue antimicrobial peptoids reported by the Seo laboratory is the sole example we found.[19] Here we report systematic studies of twenty peptoid hexamers designed to adopt amphiphilic helix structures in aqueous solution. The site-specific contributions of varied residues to the putative peptoid structure were explored. Our results reveal that the hydrophobic, aromatic residue identity and position in the sequence have the most significant effect on peptoid structure.

Twelve isomeric peptoid hexamers were initially designed and synthesized to explore the influence of residue positioning on peptoid secondary structure (**1**–**12**, Table 1). The peptoids prepared were composed of three residues: the aromatic, hydrophobic residue (*S*)-*N*-1-(naphthylethyl)glycine (*N*s1npe), *N*-[(*N*,*N*-diisopropyl)2-aminoethyl]glycine (*N*^{i}Pr$_2$ae), a polar residue expected to have a positive charge at neutral pH in aqueous solutions, and (*S*)-*N*-(1-carboxyethyl)glycine (*N*sce), expected to have a negative charge at neutral pH. Both *N*s1npe and *N*^{i}Pr$_2$ae residues have been shown to strongly favor the *cis*-amide bond conformation;[21,23] as such, we reasoned that they would be strongly PPI-helix-promoting, and the chiral *N*s1npe and *N*sce residues would enable CD spectroscopic comparisons to other peptoids. Following design principles outlined in the literature,[8,26] the putative helix was expected to display the aromatic, hydrophobic side chains on one face and the polar groups on the other two faces (see PPI helix wheel for **1** in Table 1, for other peptoids in the Supporting Information). For structural comparison, our laboratory has previously reported similar amphiphilic helical structures from 6 to 15 residues in length, including a close analogue of **5**.[27] We have observed peptoid self-association of longer, 15-residue peptoid amphiphilic PPI helices in water;[27–30] our work here focused on shorter, nonaggregating sequences.

Isomeric peptoids with predicted amphiphilic PPI helix structure were prepared that varied the specific ordering of residues. Peptoids **1**–**4** all included *N*s1npe aromatic residues at positions 1 (*N*-terminus) and 4 in the linear sequence, and they vary from one another in the ordering of the polar *N*^{i}Pr$_2$ae and *N*sce residues on the other two helix faces. Peptoids **5**–**8** all included aromatic *N*s1npe residues at positions 2 and 5 while varying the placement of the polar residues, and peptoids **9**–**12** included aromatic *N*s1npe residues at positions 3 and 6 (*C*-terminus). Solid-phase peptoid synthesis and purification were carried out following reported methods,[1,31] and peptoids' identities were confirmed by mass spectrometry (see the Supporting Information). We did not observe evidence of peptoid aggregation in aqueous solution, e.g., concentration-dependent CD or fluorescence spectral features (see the Supporting Information).

To evaluate structural differences between the peptoids and to compare them with peptoids previously synthesized by our laboratory[27,28] and others,[11,24,25] we acquired their CD spectra in a range of conditions (Figure 2).[32] Peptoid PPI helices that comprise different residues have different CD spectra, and side-chain contributions to the CD spectra often obscure the canonical peptide PPI helix CD signature.[6–12] The CD spectra of **1**–**12** are dominated by features attributed to side-chain contributions of the *N*s1npe residues.

Most notably, spectra of peptoids **1**–**4** in neutral aqueous buffer exhibited uniform features that were not observed in the spectra of **5**–**12**. CD spectra of **1**–**4** all included split maxima/minima around the naphthalene ^1B_b transition: a maximum around 220 nm and a minimum at 230 nm. These spectral features were characteristic of excitonic coupling of the two naphthalene chromophores; in excitonically coupled systems, the amplitude of the peaks and the separation of the bisignate peaks along the wavelength axis ($\Delta\square_{\text{max}}$) are correlated to the specific orientation of the coupled naphthalene dipoles.[33,34] The overlapping features in

Table 1 Isomeric Peptoids Prepared

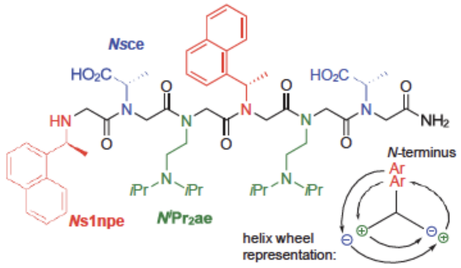

1

Peptoid	Sequence
1	*N*s1npe–*N*sce–*N*^{i}Pr$_2$ae–*N*s1npe–*N*^{i}Pr$_2$ae–*N*sce
2	*N*s1npe–*N*^{i}Pr$_2$ae–*N*sce–*N*s1npe–*N*sce–*N*^{i}Pr$_2$ae
3	*N*s1npe–*N*^{i}Pr$_2$ae–*N*^{i}Pr$_2$ae–*N*s1npe–*N*sce–*N*sce
4	*N*s1npe–*N*sce–*N*sce–*N*s1npe–*N*^{i}Pr$_2$ae–*N*^{i}Pr$_2$ae
5	*N*sce–*N*s1npe–*N*^{i}Pr$_2$ae–*N*^{i}Pr$_2$ae–*N*s1npe–*N*sce
6	*N*sce–*N*s1npe–*N*sce–*N*^{i}Pr$_2$ae–*N*s1npe–*N*^{i}Pr$_2$ae
7	*N*^{i}Pr$_2$ae–*N*s1npe–*N*sce–*N*sce–*N*s1npe–*N*^{i}Pr$_2$ae
8	*N*^{i}Pr$_2$ae–*N*s1npe–*N*^{i}Pr$_2$ae–*N*sce–*N*s1npe–*N*sce
9	*N*sce–*N*sce–*N*s1npe–*N*^{i}Pr$_2$ae–*N*^{i}Pr$_2$ae–*N*s1npe
10	*N*^{i}Pr$_2$ae–*N*sce–*N*s1npe–*N*ce–*N*^{i}Pr$_2$ae–*N*s1npe
11	*N*^{i}Pr$_2$ae–*N*^{i}Pr$_2$ae–*N*s1npe–*N*sce–*N*sce–*N*s1npe
12	*N*sce–*N*^{i}Pr$_2$ae–*N*s1npe–*N*^{i}Pr$_2$ae–*N*sce–*N*s1npe

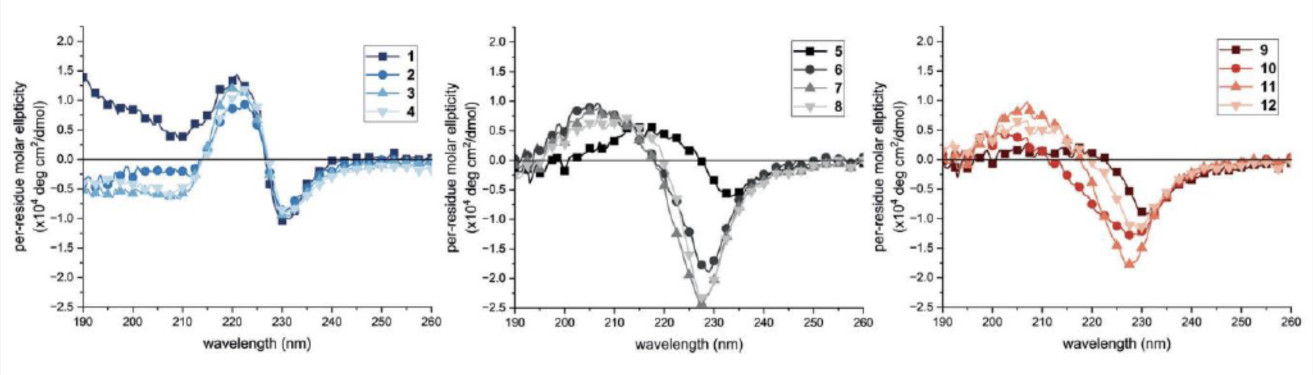

Figure 2 CD spectra of peptoids **1–12** exhibit spectral features that are dominated by side-chain interactions and that correlate with aromatic residue placement in the sequence. All peptoids were 100 ·M in 5 mM citrate-phosphate buffer, pH 7.

this region suggested that **1**–**4** all place the naphthalene side chains in a similar arrangement. Other water-soluble helical peptoids and □-peptoids bearing analogous naphthalene side chains also exhibited excitonic coupled CD features.[27,28,35] At wavelengths below 210 nm, there were no distinct spectral features, and we hypothesized that spectral differences in this region were the result of other side-chain interactions and/or backbone heterogeneity.

Most of the CD spectra of peptoid isomers without an *N*-terminal *N*s1npe residue did not show strong exciton-coupled peaks, suggesting that the internal and *C*-terminal naphthalenes have less flexibility to interact with the other aromatic group in the sequence. CD spectra of peptoids **6**–**8**, **11**, and **12** exhibited broad maxima at 207 nm and sharp minima at 227 nm (**7**, **8**, and **11**) or 229 nm (**6** and **12**). Their similar spectra suggested that dipole–dipole interactions of the naphthalene side chains in peptoids **6**–**8**, **11**, and **12** were minimized. We speculated that the broad maximum at 207 nm was analogous to the helical spectral signature of similar magnitude observed for aliphatic peptoid hexamer helices in organic solution.[24] The spectrum of **10** was unique from the others in that it exhibited a broad minimum at 227 nm and a broad maximum at 202 nm. Lastly, spectra of peptoids **5** and **9** had red-shifted minima at 233 and 231 nm, respectively, and both had broad maxima around 217 nm. Peptoids **5** and **9** share the four-residue sequence *N*s1npe-*N*^{i}Pr$_2$ae-*N*^{i}Pr$_2$ae-*N*s1npe, and we posited that this subsequence positioned the naphthalene side chains in similar conformations. None of the peptoids exhibited appreciable CD signals in the near UV wavelengths (see the Supporting Information). Additionally, we observed that CD spectra were not changed appreciably by solution pH changes, despite that the *N*^{i}Pr$_2$ae modestly favors the *trans*-amide conformation at high pH[23] (see the Supporting Information). We suggest that the *N*s1npe residues' conformations most strongly direct the peptoid PPI helix structure in aqueous solution.

The CD spectra of peptoids **1**–**12** in organic solvents, methanol, and acetonitrile, were compared. Because $K_{cis/trans}$ values are higher in organic solvents than in water,[21,23] spectral features that correlate with more helical structure were expected to be more intense in organic solvents. Correspondingly, spectral features were more intense in organic solvents for most peptoids (see the Supporting Information). The persistence of the excitonic coupling features observed in the spectra of **1**–**4** in organic solvents is unique from previous observations in longer peptoids.[27,28] We posit that the peptoid backbone conformation directed the naphthalene side-chain dipole–dipole interactions, rather than a hydrophobic effect that positioned the naphthalenes in a specific orientation.

The effects of temperature on the aqueous CD spectral features of representative peptoids were also evaluated as shown for **2** in Figure 3 (others in the Supporting Information). For all of the selected peptoids studied, CD signal intensity decreased by roughly half upon heating from 2 °C to 90 °C. This intensity change was consistent with each of these peptoids exhibiting more *cis*-*trans*-amide heteroge-

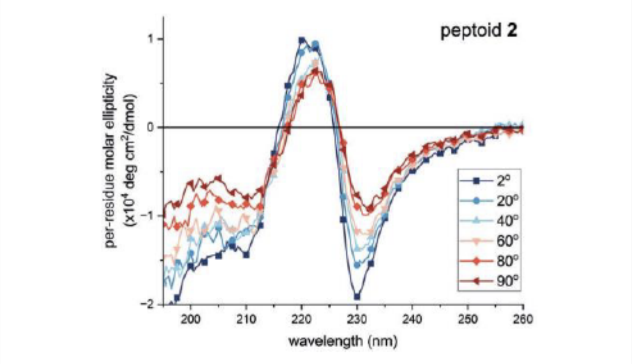

Figure 3 CD spectra of peptoid **2**, which includes an *N*-terminal *N*s1npe residue, at varied temperatures in 5 mM citrate-phosphate buffer, pH 7

neity at higher temperatures. The spectra of **2** exhibited isodichroic points at 213 nm and 225 nm over the temperature range. Because the maxima/minima wavelengths did not change, we speculated that the structural heterogeneity introduced upon heating was not accompanied by a change in electronic interactions of the *Ns*1npe side chains. No appreciable hysteresis was observed in the CD spectra when the samples were cooled to 2 °C after heating (see the Supporting Information).

Eight peptoids predicted to be less helical than **1**–**4** were subsequently designed and prepared (Table 2). These included *N*-(2-aminoethyl)glycine (*N*ae) residues (**13**–**16**) or (*S*)-*N*-2-(naphthylethyl)glycine (*Ns*2npe) residues (**17**–**20**) in lieu of N^iPr$_2$ae or *Ns*1npe, respectively. Both *N*ae and *Ns*2npe have reported $K_{cis/trans}$ values lower than those reported for N^iPr$_2$ae or *Ns*1npe.[21,23] We anticipated that these substitutions would introduce backbone structural heterogeneity, allowing us to interrogate residue-specific contributions to the structure.

Table 2 Additional Peptoids Prepared

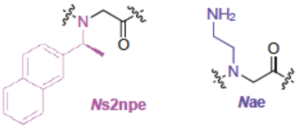

Peptoid	Sequence
13	*Ns*1npe–*N*ae–*N*sce–*Ns*1npe–*N*sce–*N*ae
14	*Ns*1npe–*N*sce–*N*ae–*Ns*1npe–*N*ae–*N*sce
15	*Ns*1npe–*N*ae–*N*ae–*Ns*1npe–*N*sce–*N*sce
16	*Ns*1npe–*N*sce–*N*sce–*Ns*1npe–*N*ae–*N*ae
17	*Ns*2npe–N^iPr$_2$ae–*N*sce–*Ns*2npe–*N*sce–N^iPr$_2$ae
18	*Ns*2npe–*N*sce–N^iPr$_2$ae–*Ns*2npe–N^iPr$_2$ae–*N*sce
19	*Ns*2npe–N^iPr$_2$ae–N^iPr$_2$ae–*Ns*2npe–*N*sce–*N*sce
20	*Ns*2npe–*N*sce–*N*sce–*Ns*2npe–N^iPr$_2$ae–N^iPr$_2$ae

CD spectra of peptoids **13**–**20** were acquired (Figure 4). In aqueous buffer at neutral pH, CD spectral features of **13**–**16** were very similar to **1**–**4**, suggesting that this residue substitution has little impact on peptoid helix structure (see the Supporting Information). In contrast, the spectral features of **17**–**20** were quite different from those of **1**–**4** (Figure 4), consistent with the unique absorbance and excitonic coupling of the 2-substituted naphthalene in the *Ns*2npe side chain relative to the *Ns*1npe naphthalene.[36] Additionally, there were many differences in peak intensities and peak wavelengths between **17**–**20**. The spectra of **17** and **20** have minima that are more than twice as intense as the minima for **18** and **19** (and **1**–**4**). Spectra of **17**, **19**, and **20** all included a minimum at 223 nm, but the minimum in **18** was at 230 nm. The spectra of **19** and **20** also included a modest shoulder minimum at 230 nm.

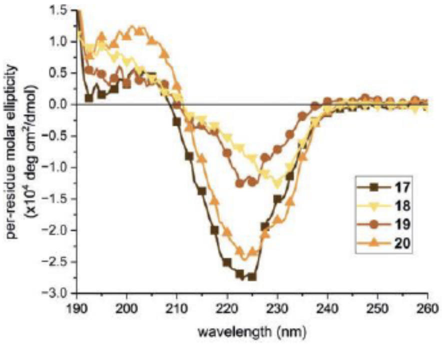

Figure 4 CD spectra of peptoids **17**–**20** in 5 mM citrate-phosphate buffer, pH 7

We interpreted the varied spectral features for **17**–**20** to be consistent with backbone conformational heterogeneity among these peptoids. Because of their different backbone conformational ensembles, peptoids **17**–**20** accessed a range of excitonic structures; the changes to minimum peak wavelengths and the presence of shoulders were evidence for these excitonic structures, rather than the bisignate spectral features observed for **1**–**4**.

Our findings here confirm that placement and identity of naphthalene-bearing residues within a peptoid hexamer influence side-chain interactions accessible within the peptoid helical structure. Specifically, we hypothesize that when the *Ns*1npe or *Ns*2npe aromatic residue is in the *N*-terminal position, the side chain has flexibility that allows it to interact with another aromatic side chain. The ordering of charged residues has a more minimal effect on the peptoid structure. Ongoing studies will examine if these observations are unique to peptoids comprising naphthalene-bearing residues. Further, we intend to use other structural studies (e.g., NMR spectroscopy) to detail the structures of these hexamers and of longer and more diversely functionalized peptoids. These results provide insights to guide the future design of short, structured, water-soluble peptoids, and will accelerate peptoids' use in a variety of biomimetic applications.

Conflict of Interest

The authors declare no conflict of interest.

Funding Information

National Science Foundation (CHE-1904991), Camille and Henry Dreyfus Foundation (Henry Dreyfus Teacher-Scholar Award to A.A.F.), Richard Bastiani (undergraduate research award to J.M.J.).

Supporting Information

Supporting information for this article is available online at https://doi.org/10.1055/a-2238-5394.

References and Notes

(1) Connolly, M. D.; Xuan, S.; Molchanova, N.; Zuckermann, R. N. *Methods Enzymol.* **2021**, *656*, 241.

(2) Zuckermann, R. N.; Kerr, J. M.; Kent, S. B. H.; Moos, W. H. *J. Am. Chem. Soc.* **1992**, *114*, 10646.

(3) Miller, S. M.; Simon, R. J.; Ng, S.; Zuckermann, R. N.; Kerr, J. M.; Moos, W. H. *Bioorg. Med. Chem. Lett.* **1994**, *4*, 2657.

(4) Astle, J. M.; Udugamasooriya, D. G.; Smallshaw, J. E.; Kodadek, T. *Int. J. Pept. Res. Ther.* **2008**, *14*, 223.

(5) Schwochert, J.; Turner, R.; Thang, M.; Berkeley, R. F.; Ponkey, A. R.; Rodriguez, K. M.; Leung, S. S. F.; Khunte, B.; Goetz, G.; Limberakis, C.; Kalgutkar, A. S.; Eng, H.; Shapiro, M. J.; Mathiowetz, A. M.; Price, D. A.; Liras, S.; Jacobson, M. P.; Lokey, R. S. *Org. Lett.* **2015**, *17*, 2928.

(6) Armand, P.; Kirshenbaum, K.; Falicov, A.; Dunbrack, R. L.; Dill, K. A.; Zuckermann, R. N.; Cohen, F. E. *Folding Des.* **1997**, *2*, 369.

(7) Wu, C. W.; Kirshenbaum, K.; Sanborn, T. J.; Patch, J. A.; Huang, K.; Dill, K. A.; Zuckermann, R. N.; Barron, A. E. *J. Am. Chem. Soc.* **2003**, *125*, 13525.

(8) Wu, C. W.; Sanborn, T. J.; Huang, K.; Zuckermann, R. N.; Barron, A. E. *J. Am. Chem. Soc.* **2001**, *123*, 6778.

(9) Gimenez, D.; Zhou, G.; Hurley, M. F. D.; Aguilar, J. A.; Voelz, V. A.; Cobb, S. L. *J. Am. Chem. Soc.* **2019**, *141*, 3430.

(10) Gimenez, D.; Aguilar, J. A.; Bromley, E. H. C.; Cobb, S. L. *Angew. Chem. Int. Ed.* **2018**, *57*, 10549.

(11) Stringer, J. R.; Crapster, J. A.; Guzei, I. A.; Blackwell, H. E. *J. Am. Chem. Soc.* **2011**, *133*, 15559.

(12) Roy, O.; Dumonteil, G.; Faure, S.; Jouffret, L.; Kriznik, A.; Taillefumier, C. *J. Am. Chem. Soc.* **2017**, *139*, 13533.

(13) Crapster, J. A.; Stringer, J. R.; Guzei, I. A.; Blackwell, H. E. *Pept. Sci.* **2011**, *96*, 604.

(14) D'Amato, A.; Pierri, G.; Tedesco, C.; Della Sala, G.; Izzo, I.; Costabile, C.; De Riccardis, F. *J. Org. Chem.* **2019**, *84*, 10911.

(15) Gorske, B. C.; Mumford, E. M.; Gerrity, C. G.; Ko, I. *J. Am. Chem. Soc.* **2017**, *139*, 8070.

(16) Crapster, J. A.; Guzei, I. A.; Blackwell, H. E. *Angew. Chem. Int. Ed.* **2013**, *52*, 5079.

(17) Robertson, E. J.; Battigelli, A.; Proulx, C.; Mannige, R. V.; Haxton, T. K.; Yun, L.; Whitelam, S.; Zuckermann, R. N. *Acc. Chem. Res.* **2016**, *49*, 379.

(18) Chongsiriwatana, N. P.; Patch, J. A.; Czyzewski, A. M.; Dohm, M. T.; Ivankin, A.; Gidalevitz, D.; Zuckermann, R. N.; Barron, A. E. *Proc. Natl. Acad. Sci. U.S.A.* **2008**, *105*, 2794.

(19) Nam, H. Y.; Choi, J.; Kumar, S. D.; Nielsen, J. E.; Kyeong, M.; Wang, S.; Kang, D.; Lee, Y.; Lee, J.; Yoon, M.-H.; Hong, S.; Lund, R.; Jenssen, H.; Shin, S. Y.; Seo, J. *ACS Infect. Dis.* **2020**, *6*, 2732.

(20) Bicker, K. L.; Cobb, S. L. *Chem. Commun.* **2020**, *56*, 11158.

(21) Gorske, B. C.; Stringer, J. R.; Bastian, B. L.; Fowler, S. A.; Blackwell, H. E. *J. Am. Chem. Soc.* **2009**, *131*, 16555.

(22) Butterfoss, G. L.; Renfrew, P. D.; Kuhlman, B.; Kirshenbaum, K.; Bonneau, R. *J. Am. Chem. Soc.* **2009**, *131*, 16798.

(23) Wijaya, A. W.; Nguyen, A. I.; Roe, L. T.; Butterfoss, G. L.; Spencer, R. K.; Li, N. K.; Zuckermann, R. N. *J. Am. Chem. Soc.* **2019**, *141*, 19436.

(24) Rzeigui, M.; Traikia, M.; Jouffret, L.; Kriznik, A.; Khiari, J.; Roy, O.; Taillefumier, C. *J. Org. Chem.* **2020**, *85*, 2190.

(25) Shin, H.-M.; Kang, C.-M.; Yoon, M.-H.; Seo, J. *Chem. Commun.* **2014**, *50*, 4465.

(26) Lee, B.-C.; Chu, T. K.; Dill, K. A.; Zuckermann, R. N. *J. Am. Chem. Soc.* **2008**, *130*, 8847.

(27) Fuller, A. A.; Yurash, B. A.; Schaumann, E. N.; Seidl, F. J. *Org. Lett.* **2013**, *15*, 5118.

(28) Fuller, A. A.; Jimenez, C. J.; Martinetto, E. K.; Moreno, J. L.; Calkins, A. L.; Dowell, K. M.; Huber, J.; McComas, K. N.; Ortega, A. *Front. Chem.* **2020**, *8*, 260.

(29) Fuller, A. A.; Huber, J.; Jimenez, C. J.; Dowell, K. M.; Hough, S.; Ortega, A.; McComas, K. N.; Kunkel, J.; Asuri, P. *Biopolymers* **2019**, *110*, e23248.

(30) Fuller, A. A.; Tenorio, K.; Huber, J.; Hough, S.; Dowell, K. M. *Supramol. Chem.* **2018**, *30*, 336.

(31) Peptoid synthesis and purification was carried out as described in ref. 28 with modifications for introduction of N^{i}Pr$_2$ae residues as described in ref. 1; additional details are provided in the Supporting Information. Purified, lyophilized peptoids were dissolved in methanol to prepare 1–2 mM stock. Concentrations were determined by UV absorbance measurements of stock solutions diluted into phosphate-buffered saline (PBS): ▭ 3200 M^{-1} cm^{-1} for **1**–**16** at 266 nm; ▭ 6359 M^{-1} cm^{-1} for **17**–**20** at 266 nm.

(32) CD spectra were acquired as described in ref. 28. Additional details are provided in the Supporting Information.

(33) Mason, S. F.; Seal, R. H.; Roberts, D. R. *Tetrahedron* **1974**, *30*, 1671.

(34) Di Bari, L.; Pescitelli, G.; Salvadori, P. *J. Am. Chem. Soc.* **1999**, *121*, 7998.

(35) Wellhöfer, I.; Frydenvang, K.; Kotesova, S.; Christiansen, A. M.; Laursen, J. S.; Olsen, C. A. *J. Org. Chem.* **2019**, *84*, 3762.

(36) Salvadori, P.; Piccolo, O.; Bertucci, C.; Menicagli, R.; Lardicci, L. *J. Am. Chem. Soc.* **1980**, *102*, 6859.